Molecule Specific Imaging of Freeze-Fractured, Frozen-Hydrated Model Membrane Systems Using Mass Spectrometry

Donald M. Cannon, Jr., Michaeleen L. Pacholski, Nicholas Winograd,* and Andrew G. Ewing*

Contribution from the Department of Chemistry, The Pennsylvania State University, 152 Davey Laboratory, University Park, Pennsylvania 16802

Received June 18, 1999

Abstract: Imaging time-of-flight secondary ion mass spectrometry is used to chemically resolve the spatial distribution of lipids in submicrometer sections of phospholipid membranes. The results show that it is possible to unravel dynamical events such as chemical fluctuations associated with domain structure in cellular membranes. In this work, a liposome model system has been used to capture the stages of membrane fusion between two merging bilayer systems. Fracturing criteria for preserving chemical distributions are shown to be much more stringent than morphological electron cryomicroscopy studies. Images of membrane heterogeneity, induced via mixing various liposomes followed by fast freezing, demonstrate the necessary sample preparation groundwork to investigate complex, heterogeneous membrane domains. Clear delineation of membrane structure provides direct evidence that specific domains or "rafts" can exist. Moreover, low concentrations of each phospholipid are distributed throughout newly fused liposomes despite the existence of distinct domains. In the liposome model, membrane structure ranges from specific domains to a fluid mosaic of the phospholipids during the fusion event. The availability of mass spectrometric imaging is proposed to facilitate the discovery of functional rafts or substructure in cell membranes before, during, and after events including cell division, exocytosis, endocytosis, intracellular transport, infection of membrane-bound viruses, and receptor clustering. This technology holds the promise to define the biology of cell membranes at the molecular level.

Introduction

Biological membranes are essential in defining cellular boundaries and sustaining cellular functions such as maintaining and conserving biological energy and providing the means for intercellular communication.[1,2] However, a lack of total understanding concerning many aspects of the vast complexity of membranes still remains, especially at the molecular level. Although membranes maintain cellular definition, the consistency of the layers has been proposed as a fluid state where membrane components can freely diffuse.[2] The simplicity of the "fluid mosaic model" has undergone an extensive evolution.[3−9] It is reasonable to assume that the high level of diversity among lipids (i.e., backbones, headgroups, fatty acid size, or degree of unsaturation) is to allow membrane form to meet cellular function. Indeed, it has been shown that there is chemical heterogeneity, not only across the bilayer[3,4] but within a specific layer as well.[5−9]

Membranes are now recognized to contain numerous domains with restricted diffusion of their components in order to influence cellular shape or to carry out a cellular function. Chemical domains such as these have been termed "rafts" in the lipid membrane as they are thought to carry structures to specific sites on the cell and, thus, are of fundamental importance to cell biology.[9] Many cellular functions, such as fusion and fission, rely on membrane dynamics. Biological examples of these membrane dynamics include exocytosis for fusion and endocytosis or mitosis for fission. Exocytosis and endocytosis are membrane processes involved in the interaction of the cell with its surroundings. It is now accepted that the uniqueness and diversity of cellular functions arise from membrane fluidity as well as localized domains of confined fluidity that further create heterogeneity within cellular membranes. However, it is still unclear whether chemical heterogeneity between the two merging or diverging membranes drives these membrane processes.[10]

Because of the noncovalent structure of membranes, most tools used in membrane investigations involve indirect analysis methods that either do not target individual cells or only give a topographical view with little or no chemical information. Earlier chemical composition studies have shown a higher percentage of lipids with unsaturated fatty acid tail groups associated with axons versus the cell body, possibly for providing a more disordered axonal membrane structure necessary for a large number of quick fusion processes.[11] Studies of

(1) *Biochemistry of Lipids, Lipoproteins and Membranes, New Comprehensive Biochemistry;* Vance, D. E., Vance, J. E., Eds.; Elsevier Science Publishing Co., Inc: New York, 1991; Vol. 20.
(2) Singer, S. J.; Nicolson, G. L. *Science* **1972**, *175*, 720−730.
(3) Rothman, J. E.; Lenard, J. *Science* **1977**, *195*, 743−753.
(4) Fujimoto, K.; Umeda, M.; Fujimoo, T. *J. Cell Sci.* **1996**, *109*, 2453−2460.
(5) Glaser, M. *Curr. Opin. Struct. Biol.* **1993**, *3*, 475−481.
(6) Kobayashi, T.; Storrie, B.; Simons, K.; Dotti C. G. *Nature* **1992**, *359*, 647−650.
(7) Nelson, W. J. *Science* **1992**, *258*, 948−955.
(8) Thompson, T. E.; Sankaram, M. B.; Biltonen, R. L. *Comments Mol. Cell Biophys.* **1992**, *8*, 1−15.
(9) Simons, K.; Ikonen, E. *Nature* **1997**, *387*, 569−572.
(10) Knoll, G.; Plattner, H. In *Electron Microscopy of Subcellular Dynamics*; Plattner, H., Ed.; CRC Press: Boca Raton, FL, 1989; Chapter 6.
(11) Cullis, P. R.; Hope, M. J. In *Biochemistry of Lipids, Lipoproteins and Membranes, New Comprehensive Biochemistry*; Vance, D. E., Vance, J. E., Eds.; Elsevier Science Publishing Co., Inc: New York, 1991; Vol. 20, pp 1−41.

10.1021/ja992078p CCC: $19.00
Published on Web 01/15/2000

membrane dynamics with electron microscopy have used freeze-drying and cryoprotectant preparations that have shown a clearing of intramembrane proteins (IMPs) associated with exocytosis.[10,12] However, more recent fast-freezing preparation studies have shown results more consistent with the physiology of exocytosis and found no clearing of IMPs.[12] Current methods aimed at spatially localizing and imaging the chemical structure of cellular membranes at the single-cell level include patch clamp,[13] fluorescence recovery after photobleaching,[14] near-field optical microscopy,[15] and a combination of neutron diffraction and atomic force microscopy.[16] Despite limitations of these various techniques, these investigations have provided a vast amount of valuable knowledge about membrane domains and strongly suggest involvement of lipid chemical heterogeneity in membrane dynamics. Our laboratories are interested in developing probes of native domain structure in cell membranes. Probes employed in fluorescence techniques have been known to change domain structure induced in Langmuir−Blodgett (LB) model membranes.[17,18] Thus, a method that does not require phospholipid labeling appears to be necessary for the study of domain structure in membranes.

There have been substantial efforts by the secondary ion mass spectrometry (SIMS) community concerning the chemical imaging of biological systems.[19,20] Briefly, SIMS involves bombardment of a sample surface with a primary ion beam resulting in ejection (sputtering) of electrons and neutral or ionized atoms and/or molecules from the surface.[21] The secondary ions are focused into a mass analyzer for a mass-to-charge spectrum of the surface species. Dynamic SIMS utilizes a high-flux primary ion beam ($>1 \times 10^{13}$ primary ions/cm^2) to probe many layers into the solid, thus creating significant damage and limiting the amount of molecular information. Dynamic SIMS has been used to probe the spatial distribution of atomic and small molecular fragment ions at or near biological surfaces.[22−26] With technological advancements increasing the sensitivity of mass analyzers, namely, the development of the time-of-flight (TOF) analyzer,[27] an extremely surface sensitive analysis is obtained in the static SIMS regime.[18,28−31] Static SIMS ($<10^{13}$ primary ions/cm^2, defined as sampling equal to or less than 1% of the first monolayer) probes the molecules at the top layer of a relatively undisturbed surface. This maximizes the quality and quantity of molecular information obtained by significantly reducing fragmentation of sputtered ions, while permitting spatial analysis of smaller membrane areas than have been measured with other techniques.

Imaging static TOF-SIMS utilizes a 20−100-ns pulse of a focused ion beam probe with a size of approximately 200 nm to desorb surface molecules into the TOF analyzer.[21,30−33] By rastering the probe over the specimen and collecting mass spectra at each position, molecule-specific images of particular masses can be reconstructed. Static TOF-SIMS analyses of membrane systems have been successfully employed in our laboratories for preliminary experiments on LB films and single cells.[30,33] Early single-cell studies have demonstrated the capability of this technique for molecular imaging of lipophilic dopants such as dimethyl sulfoxide and cocaine.[30] However, no native membrane chemicals had yet been identified and only low-mass hydrocarbon fragments had been successfully imaged. It is likely that sample preparation issues had been responsible for this lack of chemical information. To test this hypothesis, we have employed multilamellar liposomes to systematically vary the techniques required for analysis of frozen-hydrated, freeze-fractured biological membranes[31] and they are described in more detail here. These systematic studies have led to protocols that allow various membrane components to be directly detected. More recently, TOF-SIMS analyses of LB films and red blood cells have shown the ability of this technique to provide an orientation signature for lipid molecules that are exposed on the surface.[33]

Static imaging TOF-SIMS is a surface-sensitive probe performed in an ultrahigh vacuum (UHV) environment ($\sim 10^{-10}$ Torr). Direct molecule-specific imaging of single cells with TOF-SIMS requires development of sample preparation protocols based on proven electron cryomicroscopy methods[12] adapted to optimize measurements of the top molecular layer of the sample.[23,30,31,33,34] Samples investigated by freeze-drying have documented analysis artifacts such as chemical migration and reduction of cell size due to dehydration.[23,34−36] Times for freeze-drying are longer than many cellular processes, therefore restricting the study of dynamic cellular events.[12] Conversely, fast-freezing methods have shown fewer artifacts and have been the method of choice for recent electron microscopy studies.[12] Liquid propane freezing[37] allows an entire small sample to be completely frozen in the millisecond time scale to preserve chemical spatial integrity and to reduce ice crystal damage[38] to below the resolution capabilities of TOF-SIMS. These fast-freezing times are sufficient to stop dynamic membrane events,

(12) *Rapid Freezing, Freeze-Fracture, and Deep Etching*; Severs, N., Shotton, D.; Eds.; Wiley-Liss: New York, 1995.
(13) Harder, T.; Scheiffele, P.; Verkade, P.; Simons, K. *J. Cell. Biol.* **1998**, *141*, 929−942.
(14) Schutz, G. J.; Schindler, H.; Schmidt, T. *Biophys. J.* **1997**, *73*, 1073−1080.
(15) Hwang, J.; Gherber, L. A.; Margolis, L.; Edidin, M. *Biophys J.* **1998**, *74*, 2184−2190.
(16) Gliss C.; Clausen-Schaumann, H.; Gunther, R.; Odenbach, S.; Randl, O.; Bayer, T. M. *Biophys J.* **1998**, *74*, 2443−2450.
(17) Leonard-Latour, M.; Morelis, R. M.; Coulet, P. R. *Langmuir* **1996**, *12*, 4797−4802.
(18) Leufgen, K. M.; Rulle, H.; Galla, H.-J.; Sieber, M.; Benninghoven, A. In *Secondary Ion Mass Spectrometry (SIMS X);* Benninghoven, A., Hagenhoff, B., Werner, H. W., Eds.; Wiley: New York, 1995; pp 957−960.
(19) *Biol. Cell* **1992**, *74* (1) (entire volume).
(20) Todd P. J.; McMahon J. M.; Short R. T.; McCandlish C. A. *Anal. Chem.* **1997**, *69*, 529A−535A.
(21) Winograd, N. *Anal. Chem.* **1993**, *65*, 622A−629A.
(22) Mantus, D. S.; Morrison, G. H. *Mikrochim. Acta [Wien]* **1991**, *II*, 515−522.
(23) Ausserer, W. A.; Chandra, S.; & Morrison, G. H. *J. Microsc*. **1989**, *154* (Part 1), 39−57.
(24) Smith, D. R.; Chandra, S.; Coderre, J. A.; Morrison, G. H. *Cancer Res.* **1996**, *56*, 4302−4306.
(25) Levi-Setti, R.; Chabala, J. M.; Gavrilov. K.; Espinosa, R.; LeBeau, M. M. *Cell. Mol. Biol.* **1996**, *42*, 301−324.
(26) Lazof, D. B.; Goldsmith, J. G.; Suggs, C.; Rufty, T. W.; Linton, R. W. *J. Microsc.* **1994**, *176*, 99−109.
(27) Chait, B. T.; Standing, K. G. *Int. J. Mass Spectrom. Ion Phys.* **1981**, *40*, 185−193.
(28) Briggs D.; Brown A.; Vickerman J. C. *Handbook of Static Secondary Ion Mass Spectrometry*; John Wiley & Sons: New York, 1989.
(29) John, C. M.; Odom, R. W. *Int. J. Mass Spectrom. Ion Processes* **1997**, *161*, 47−67.
(30) Colliver T. L.; Brummel C. L.; Pacholski M. L.; Swanek F. D.; Ewing A. G.; Winograd N. *Anal. Chem.* **1997**, *69*, 2225−2231.
(31) Cannon, D. M., Jr.; Pacholski, M. L.; Ewing, A. G.; Winograd, N. In *Secondary Ion Mass Spectrometry (SIMS XI)*; Gillen, G., Lareau, R., Bennett, J., Stevie, F., Eds.: Wiley: New York, 1997; pp 489−492.
(32) Levi-Setti, R.; Hallegot, P.; Girod, C.; Chabala, J. M.; Li, J.; Sodonis, A.; Wolbach, W. *Surf. Sci.* **1991**, *246*, 94−106.
(33) Pacholski, M. L.; Cannon, D. M., Jr.; Ewing A. G.; Winograd, N. *J. Am. Chem. Soc.* **1999**, *121*, 4716−4717.
(34) Chandra, S.; Bernius, M. T.; Morrison, G. H. *Anal. Chem.* **1986**, *58*, 493−496.
(35) Edelmann, L. *Scanning Microsc.* **1994**, *(*Suppl. 8), 67−81.
(36) Kachar, B.; Serrano, J. A.; Pinto da Silva P. *Cell Biol. Int. Rep.* **1980**, *4*, 347−356.
(37) Ryan, K. P.; Bald, W. B.; Neumann, K.; Simonsberger, P.; Purse, D. H.; Nicholson, D. N. *J. Microsc*. **1990**, *158* (3), 365−378.
(38) Stephenson, J. L. *J. Biophys. Biochem. Cytol*. **1956**, *2*, 45−52.

preserving a snapshot in time for analysis of the molecular spatial distribution.

In this paper, imaging static TOF-SIMS is utilized to directly measure the chemical and spatial distribution of lipid molecules on the surface of single multilamellar, micrometer-size liposomes. Imaging is achieved by probing the inner portion of a sample, frozen as a sandwich, that has been fractured in vacuo to preserve a clean fracture surface. The major goal of the fracturing event in TOF-SIMS imaging studies is simply to provide a clean surface for analysis. This is in contrast to electron microscopy studies that tailor the fracturing to occur in the median of a bilayer in order to examine internal components. Fracturing is done at a precise temperature that is pressure dependent to equilibrate the condensation and sublimation fluxes of water. Freeze fracture at a precise temperature preserves the chemical integrity by eliminating both excess water leaving the surface and the need for further surface treatments to remove water such as temperature[12] or ion etching.[34] We show that molecule-specific TOF-SIMS imaging requires more stringent temperature control versus morphological imaging using electron cryomicroscopy. A 15 °C temperature window is sufficient to demonstrate fracturing extremes ranging from total water coverage to etching that disturbs the molecular spatial integrity. Data from liposome model systems show that fusion of simple membranes involves several stages. These include initial contact, formation of specific domains with initial distribution of a small portion of the phospholipids, and then eventually a final redistribution and equilibration of the lipids to a homogeneous, fluid mosaic structure.

Experimental Section

TOF-SIMS Instrumentation. All analyses were performed on a Kratos (Manchester, U.K.) Prism TOF−SIMS spectrometer equipped with a gallium liquid metal ion gun (LMIG; FEI Co., Beaverton, OR) with a pulsed 25-kV, 500-pA beam focused 45° incident onto the sample to a 200-nm spot (described in detail elsewhere[39]). A liquid nitrogen (LN_2)-cooled stage (Kore Tech. Ltd., Cambridge, U.K.) was biased at ±2.5 kV with an extraction lens, biased at ∓4.7 kV. The horizontal time-of-flight path length was 4.5 m in length and equipped with a reflectron and a microchannel plate detector (Gallileo Co., Sturbridge, MA). Mass resolution of this instrument was typically 4000 at 200 *m*/*z* with a 50% transmission efficiency. Charge compensation was accomplished by pulsing an electron flood gun beam of 30-eV electrons for 50 μs after each LMIG pulse. Imaging was accomplished by rastering the primary ion beam over the surface while collecting the corresponding TOF spectra for each point to generate a pixel image of selected ions. The area of TOF-SIMS analysis was correlated to a 400× microscope optical image, thus allowing the sample surface to be optically surveyed before analysis. The instrument was also equipped with a channeltron detector capable of recording scanning ion micrographs analogous to scanning electron micrographs. Ion micrographs included both sputtered particles and electrons and were taken after analysis since extensive beam damage is induced by a high-flux dc (nonpulsed) ion beam.

Liposome Sample Preparation. Phospholipid and cholesterol samples were obtained from Sigma (St. Louis, MO) and Fluka (Ronkonkoma, NY) and used without further purification. Standard spectra were obtained by dissolving the compound in a volatile organic solvent, placing a small aliquot (5 μL) on a standard substrate (Si or Au), and allowing evaporation to dryness before insertion into vacuum. Multilamellar, micrometer-sized liposomes were formed by a rotary evaporation technique.[40] Briefly, a few milligrams of phospholipid/cholesterol (a ∼1:1 molar ratio) were dissolved in an organic solvent, typically chloroform, and placed into a round-bottom evaporator flask. The flask was then rotated while a vacuum was drawn, creating an even coating of the flask. Water (∼20 mL) was then added and swirled to resuspend the phospholipid/cholesterol coating into water-soluble structures such as multilamellar liposomes. Different phospholipids and cholesterol were used for liposomes of mixed compositions. Liposome formation was verified by optical microscopy. A small drop (3−10 μL) of liposome suspension is placed on a 5 × 5 mm silicon wafer (Ted Pella Inc., Redding, CA). A smaller shard of Si was placed across the diagonal, on top of the liposome suspension to form the sample sandwich (Figure 1). This sandwich was then immersed into liquid propane for several seconds and then stored in LN_2.

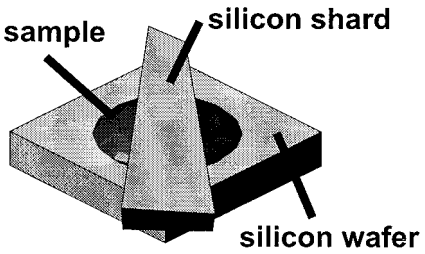

Figure 1. Schematic of the sandwich sample preparation. A small drop (3−10 μL) of liposome suspension is placed on a 5 × 5 mm silicon wafer. A smaller silicon shard is placed across the diagonal, on top of the suspension, to form the sample sandwich. This construct is then rapidly frozen in liquid propane.

Liposome Mixing. Time-resolved analysis was accomplished by fast freezing in liquid propane at given time intervals after the mixing step. Mixing simply involved taking two vials of separate liposome suspensions and mixing them into a third vial. Approximately 5 μL of the resulting suspension was then quickly placed between two silicon pieces to be frozen as fast as 30 s after mixing.

Freeze-Fracture Instrumentation. The complete cold chain freeze-fracture method has been described in detail elsewhere[30] and is briefly described here. Samples were removed from the LN_2 storage vessel and mounted onto a copper sample block with screws while under LN_2. The load lock chamber was then vented to atmosphere pressure with dry nitrogen gas, allowing the vertical sample arm to be immersed into a LN_2 dewar below. The sample block was then placed onto the vertical sample arm under LN_2. This sample arm was quickly raised into the chamber where vacuum base pressures of 10^{-7} Torr were achieved with two turbomolecular pumps (230 and 170 L/s, Pfeiffer Vacuum Technology, Inc., Nashua, NH), backed by a rough pump (Edwards Vacuum Technology, Inc., West Sussex, U.K.). A thermocouple wire mounted on the vertical sample arm directly behind the sample and an ion pressure gauge were used to monitor the sample temperature and pressure, respectively. Once at a given temperature and pressure, a LN_2-cooled knife was manipulated to quickly pry off the top shard of the sample sandwich. The LN_2-cooled horizontal transfer arm was placed in the immediate vicinity to scavenge water from the fracturing process. Once the sample was fractured, the knife was withdrawn and the sample was transferred to the horizontal transfer arm where it delivered the sample through a gate valve to the liquid nitrogen-cooled stage in the analysis chamber.

Safety Considerations. Liquid propane was created for these experiments in an explosion proof hood by condensing propane gas from a cylinder while stirring with a magnetic stirrer into a plastic beaker suspended in LN_2.[41] Propane gas is extremely flammable. In addition, liquid propane can condense molecular oxygen onto the surface to form an extremely combustible mixture. Care was taken to stir the solution so as not to solidify the propane.

Results and Discussion

Molecule-Specific Mass Spectrometric Assignments. Phosphatidylcholine (PC), phosphatidyl-*N*-monomethylethanolamine (PNME), and phosphatidyldimethylethanolamine (PDME) are

(39) Wood, M.; Zhou, Y.; Brummel, C. L.; Winograd, N. *Anal. Chem.* **1994**, *66*, 2425−2432.

(40) Kates, M. In *Laboratory Techniques in Biochemistry and Molecular Biology*, 2nd ed.; Burdon, R. H., van Knippenberg, P. H., Eds.; Elsevier Science Publishing Co., Inc.: New York, 1996; Vol. 3.

(41) Ryan, K. P.; Liddicoat, M. I. *J. Microsc.* **1987**, *147* (3), 337−340.

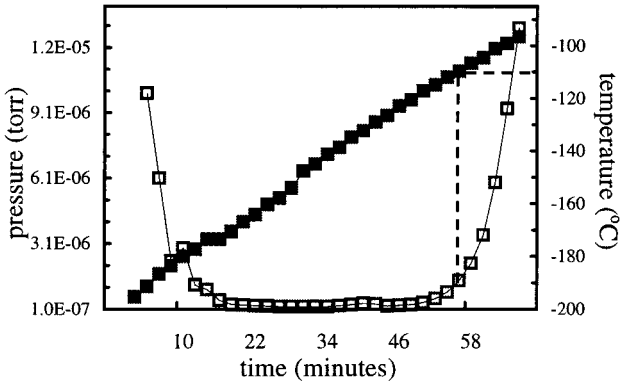

Figure 2. Average pressure and temperature versus time for the load lock system described in the text. Fracturing temperatures estimated from this plot are in the range of −115 to −110 °C for these pressures. Legend: closed, temperature; open , pressure.

used as representative glycerophospholipids for imaging. Each has characteristic headgroups attached to a glycerol backbone through a phosphate linkage. Two fatty acid nonpolar tail groups that can have a variety of lengths as well as degrees of saturation are linked to the glycerol backbone via an ester linkage. Phosphorylated headgroups (i.e., PC headgroup 184 *m*/*z*) and various tail groups (i.e., monoglyceride and diglyceride ions) have fragmentation patterns that have been reported with other mass spectrometry techniques.[42,43] TOF-SIMS spectra of standard lipid samples show characteristic ion fragments in the mass spectrum as expected. This confirms that chemical differentiation can be accomplished for relatively large molecules (600−900 Da) differing by only one methyl group.

Cholesterol is a widely studied lipid membrane sterol that is found in all eukaryoic cells. It is known to influence membrane fluidity as well as to form domains of 2:1 phospholipid/cholesterol structures.[44] TOF-SIMS spectra of cholesterol standards show two intense characteristic peaks corresponding to a cholesterol molecular ion (M^+, 386 *m*/*z*) and a fragment ion that loses the hydroxyl group ($[M - OH]^+$, 369 *m*/*z*).[33] These largely intact fragments are sufficient for chemical differentiation from the glycerophospholipids.

Freeze-Fracture Methodology. Sample temperature during fracturing needs to be optimized to preserve the hydrated sample state and to minimize interference from water deposition.[12] The critical factor is the water sublimation temperature at a given pressure. Average temperature and pressure profiles as a function of time for the load lock system described above are shown in Figure 2. The sample enters the vacuum at LN_2 temperature and slowly increases over time due mainly to heat loss through the rod of the arm. As the temperature increases, the probability of significant sublimation also increases. Monitoring the pressure profile provides a measurement related to the amount of sublimation. The pressure profile shows the time required to achieve base pressures is on the order of tens of minutes and occurs before the sample temperature is warm enough to experience water sublimation. Later, the pressure shows an appreciable increase due to significant water sublimation as the sample temperature warms above −110 °C. To equilibrate the condensation and sublimation fluxes, the optimal fracturing temperature would be just before significant sublimation is observed and is estimated from this graph to be in the range of −115 to −110 °C for these given pressures.

(42) Murphy, R. C. *Handbook of Lipid Research, Mass Spectrometry of Lipids*; Plenum Press: New York, 1993; Vol. 7, Chapter 7.
(43) Cole, M. J.; Enke, C. G. *Anal. Chem.* **1991**, *63*, 1032−1038.
(44) Engelman, D. M.; Rothman, J. E. *J. Biol. Chem.* **1972**, *247*, 3694−3697.

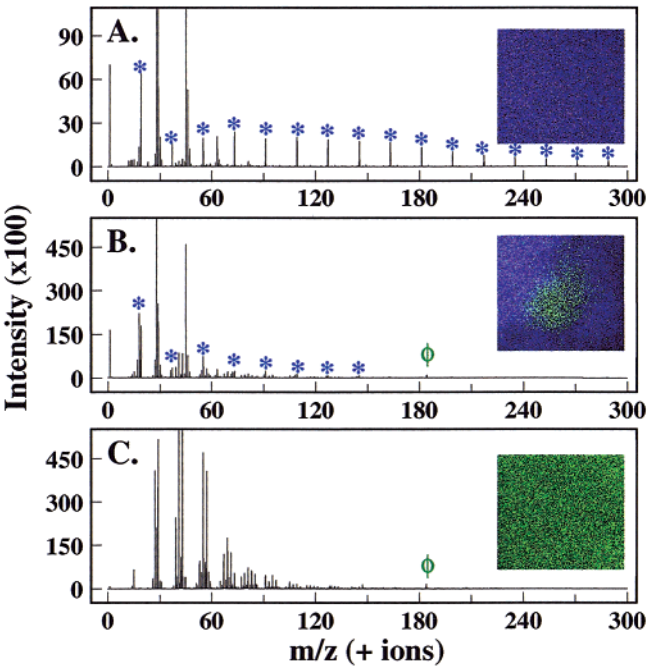

Figure 3. Positive ion TOF−SIMS spectra and images as a function of fracture temperature for three representative freeze-fractured dipalmitoylphosphatidylcholine liposome samples. Peaks labeled with an asterisk are due to the series of water clusters with the formula $[H(H_2O)_n]^+$. Major peak assignments (17.9−19.1 *m*/*z*, water, blue; 184.0−184.5 *m*/*z*, phosphocholine headgroup, green, ϕ). All images are 152 × 148 pixels in a 100-μm-wide fov. (A) Fracture temperature −110 °C. This resulted in spectra and image dominated by water and water clusters (∗); 2.4×10^{12} ions/cm^2. (B) Fracture temperature −105 °C. The localized headgroup signal demonstrates the optimum temperature for these pressures. Water clusters (∗) evident in the mass spectra indicate frozen-hydrated state; 3.2×10^{12} ions/cm^2. (C) Fracture temperature −95 °C. The absence of water clusters (∗) and the nonlocalized headgroup signal indicates significant sublimation has resulted in surface displacement; 9.2×10^{12} ions/cm^2.

Mass spectra and molecule-specific images (water, blue; phosphocholine headgroup, green (ϕ)) as a function of fracturing temperature for three representative freeze-fractured liposome samples are shown in Figure 3. When sample temperature is too cold during fracturing, water immediately condenses back on the freshly exposed surface, dramatically reducing or masking the intensity of the ions of interest. Colder temperatures (Figure 3A, −110 °C) result in spectra dominated by water clusters (∗) indicative of recondensed water on a sample surface thin enough not to experience significant charging. The image in Figure 3A shows homogeneous coverage of water on the surface probed by TOF-SIMS, even though a liposome has been optically identified in the TOF-SIMS imaging field of view (fov). When the sample temperature is too warm during fracturing, most, if not all, of the surface water is sublimed away. A 15 °C increase in fracturing temperature results in no detectable water clusters (Figure 3C). However, a characteristic hydrocarbon fragmentation pattern along with phosphorylated headgroup (phosphocholine 184 *m*/*z*) is observed where a liposome has been identified optically. In this case, phospholipid chemical images are homogeneous, suggesting that significant water sublimation ruptures liposomes from the inner aqueous core and causes movement of phospholipid molecules on the surface. "Water vapor wind phenomena" have been speculated to result from significant water sublimation fluxes large enough to sweep molecules appreciable distances across surfaces.[12] This work shows small differences in fracturing temperature can cause

uniform distributions from this water vapor wind phenomenon analogous to artifacts observed in freeze-drying preparations.[23,34−36] As demonstrated in Figure 3B, the optimum temperature for this pressure is approximately −105 °C. Water clusters are evident in the mass spectra along with characteristic hydrocarbon fragments including the phosphorylated headgroup. Previous studies have suggested that this temperature is low enough to prevent diffusion or migration of localized compounds and high enough to prevent condensation of adventitious sources of water back onto the sample surface.[30,31] The molecule-specific image of the headgroup fragment overlaid on water in Figure 3B demonstrates the feasibility of imaging spatially localized chemical structures in a frozen-hydrated membrane.

Studies utilizing electron microscopy still have not completely determined the effect of temperature on the fracturing process but have recognized water fluxes to be a dominant force.[12] Except during fracturing, residual water concentrations are kept minimal at ultrahigh vacuum pressures such that several hours are required before appreciable TOF-SIMS interference from water condensation is observed at LN_2 temperatures. This enables the sample temperature to be lowered back down to LN_2 temperature after fracturing to minimize surface damage during ion beam analysis and sublimation of surface components. The estimated fracturing temperature (Figure 2) is colder than the optimal temperature demonstrated by TOF-SIMS spectra and images (Figure 3). To obtain localized molecule-specific TOF-SIMS images, fracturing is performed after a slight pressure rise in the fracturing chamber and is typically accompanied by a subsecond transient pressure spike. These observations suggest that the act of fracturing is violent in nature, thus creating high, localized partial pressures of water at the fracture surface. Small additional sublimation fluxes, past that of equilibrated condensation and sublimation fluxes, are required to expeditiously move the localized water away from the fracture surface to avoid condensation on the fracture surface. The goal of providing a clean, undisturbed fracture surface in vacuo involves equilibrating the condensation and sublimation fluxes at the sample surface just *after* fracturing.

Fractured Surfaces. Scanning ion micrographs of the surface are a means to correlate surface morphology with chemical morphology. Ion micrographs depict surface morphology by utilizing the ion beam in a nonpulsed mode to create a high flux of sputtered ions and electrons that are subsequently detected by a channeltron detector. The high flux associated with this method destroys the chemical integrity of the surface due to high fragmentation and surface charging and thus must be done after TOF-SIMS analysis. Nevertheless, ion micrographs can track not only the surface morphology but also the conducting nature of the surface that the ion beam probes. Optically observing liposomes in ice does not indicate surface exposure. Therefore, ion micrographs are used to relate optical images to the corresponding TOF-SIMS images.

Two representative large-fov ion micrographs and one optical micrograph of surfaces that demonstrated localized molecule-specific imaging are shown in Figure 4. Large areas of exposed silicon substrate, noticed in Figure 4A as higher conducting areas (brighter intensity), are surrounded by fractured areas of ice (lower intensities) in a bricklike pattern. Localized liposome structures are observed within the areas of exposed silicon. The ion beam is incident from the right side of the image creating artifacts in the form of shadows primarily due to secondary electron emission. Secondary ion shadows are not as distinct and can be compensated for in secondary ion analysis as has been shown by TOF-SIMS imaging of polystyrene beads.[45] TOF-SIMS images of small-mass hydrocarbons are also good indicators of surface morphology and are essential in differentiating between topographical and chemical heterogeneity within biological samples. As shown in Figure 4B, liposome structures that are embedded in ice can be exposed to the ion

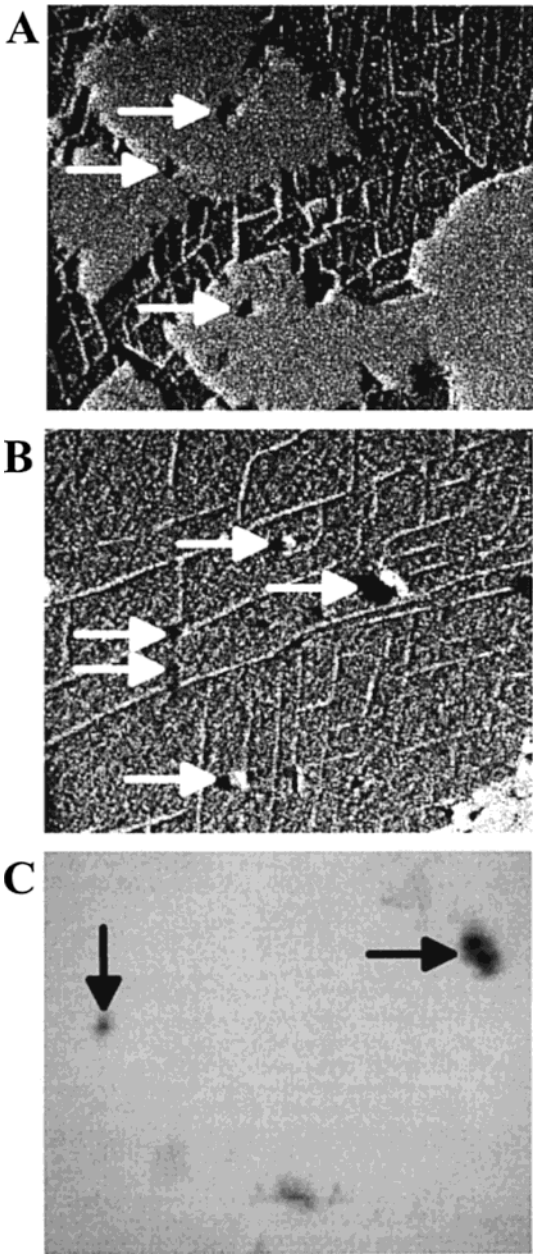

Figure 4. Representative micrographs of freeze-fractured, frozen-hydrated DPPDME/cholesterol samples that demonstrate localized molecule-specific imaging. (A) Ion micrograph of large areas of exposed silicon substrate, noticed as higher conducting areas (brighter intensity), are surrounded by fractured areas of low-conducting ice (lower intensities) in a bricklike pattern. Localized liposome structures (indicated by arrows) can be seen within the areas of exposed silicon. The ion beam is coming in from the right side of the image creating image artifacts in the form of shadows; 500-μm-wide fov. (B) Ion micrograph of liposome structures (indicated by arrows) embedded in ice but are exposed to the ion beam with clear evidence of shadowing; 333-μm-wide fov. (C) Optical micrograph of liposome structures (indicated by arrows) on an exposed silicon area; 500-μm-wide fov.

(45) Brummel, C. L.; Vickerman, J. C.; Carr, S. A.; Hemling, M. E.; Roberts, G. D.; Johnson, W.; Weinstock, J.; Gaitanopoulos, D.; Benkovic, S. J.; Winograd, N. *Anasl. Chem.* **1996**, *68*, 237−242.

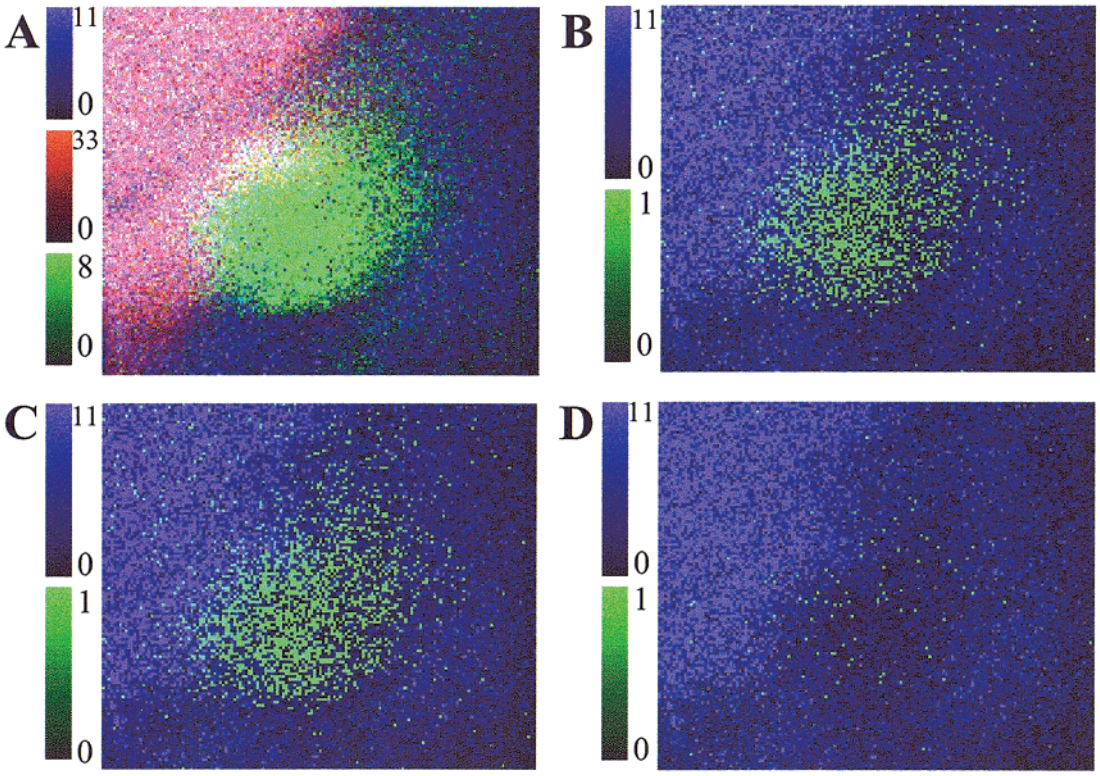

Figure 5. Positive ion TOF-SIMS images of a DPPC/cholesterol liposome on the edge of an exposed silicon area. All images are 100-μm-wide fov, 152 × 148 pixels. and 3.2×10^{12} ions/cm^2. Color equivalent intensity scales are left of the images with respective intensity ranges indicated. (A) Overlay of water (17.9−19.1 *m*/*z*; blue), silicon (27.7−28.0 *m*/*z*; red), and a C_3 hydrocarbon set (40.9−43.3 *m*/*z* 1; green). (B) Overlay of water (17.9−19.1 *m*/*z*; blue) and phosphocholine headgroup (184.0−184.4 *m*/*z*; green). (C) Overlay of water (17.9−19.1 *m*/*z*; blue) and cholesterol molecular ion (M^+, 384.0−387.0 *m*/*z*; green). (D). Overlay of water (17.9−19.1 *m*/*z*; blue) and DPPC molecular ion ($(M + H)^+$, 734.0−734.6 *m*/*z*; green).

beam with clear evidence of shadowing. Liposomes on exposed silicon and in ice both result in molecule-specific TOF-SIMS image localization. However, due to charge dissipation factors, liposomes on the exposed silicon areas give higher TOF-SIMS intensities. It is important to note, the goal of fracturing in many electron microscopy studies is to split through the middle of a membrane bilayer. A representative optical micrograph of liposome structures located in the exposed silicon parts and demonstrates the ability to optically target structures of interest before TOF-SIMS analysis is shown in Figure 4C.

Molecule-Specific Images of Liposomes. Molecule-specific TOF-SIMS images of a single freeze-fractured, frozen-hydrated dipalmitoylphosphatidylcholine (DPPC)/cholesterol liposome residing at the exposed silicon/ice-covered interface are shown in Figure 5. This picture demonstrates molecular localization is not the result of exposing the silicon substrate with phospholipid contaminants within a large structure of ice. An overlay of water (18, 19 *m*/*z*; blue), silicon (28 *m*/*z*; red), and a C_3 hydrocarbon set (41, 43 *m*/*z*; green) is presented in Figure 5A. The localized hydrocarbon signal appears in both the exposed silicon areas and the ice-covered areas. This overlay image shows that the underlying silicon substrate, when exposed, does not result in significant nonlocalized signal from the phospholipid. The signal for the phosphorylated choline headgroup (184 *m*/*z*; green) overlaid with water (18, 19 *m*/*z*; blue) in Figure 5B more clearly demonstrates the localization of membrane structure to the very edge of the exposed silicon substrate. It is interesting to note that the highest water intensities are associated with exposed silicon areas, indicative of a water layer thin enough to experience minimal charging compared to bulk ice areas. Surface topography effects, such as just described, are commonly seen and are easily discerned from the chemical heterogeneity effects as seen with the phosphocholine headgroup signal.

The average case of molecular ion intensities achieved on frozen-hydrated samples is represented in part C and D of Figure 5. The molecular ion for cholesterol (386 *m*/*z*; green) overlaid again with water (18, 19 *m*/*z*; blue) is presented in Figure 5C to demonstrate that this sterol can be localized with TOF-SIMS in a membrane structure. The image for the phosphatidylcholine dipalmitoyl molecular ion overlaid with water is presented in Figure 5D. Much higher intensities for these molecular ions have been observed, but not on a repetitive basis. Although single counts are observed for individual pixels in these images, the collected number of counts across the image is clearly meaningful statistically and is well above the baseline noise in the spectrum. It is also important to note that the intensity scale upper limit signifies pixels with equal to or greater than the indicated intensity. Therefore, even though the intensity scale indicates an upper limit of 1, pixels could contain numerous counts. As demonstrated in Figure 5D, proper freeze-fracturing of a membrane results in all of the overlying water being removed to reveal the membrane structure. Thus, the water image for this data set is an excellent example that shows both surface topography (increased signal in the upper left) and chemical morphology (decreased signal associated with the membrane structure) effects.

Liposome Mixing. Mixed liposomes demonstrate identification of several phospholipid fragments and molecular ions spatially localized within a model structure. The mass spectrum from a liposome sample containing cholesterol and two different glycerophospholipids (DPPC and dipalmitoylphosphatidyl-*N*-monomethylethanolamine (DPPNME)) is shown in Figure 6.

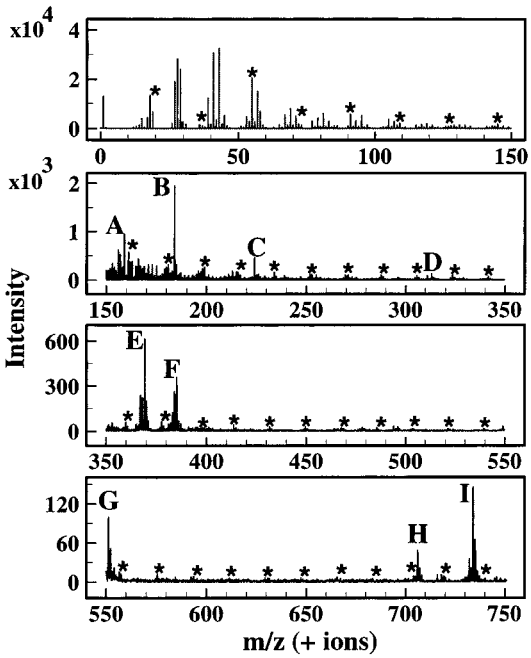

Figure 6. Representative positive ion TOF-SIMS spectrum of freeze-fractured, frozen-hydrated DPPC/cholesterol liposomes mixed with DPPNME/cholesterol liposomes. Peaks labeled with an asterisk are due to the series of water clusters with the formula $[H(H_2O)_n]^+$. Major peak assignments for the following nominal *m*/*z* species: (A) 156, phospho-*N*-monomethylethanolamine headgroup; (B) 184, phosphocholine headgroup; (C) 224, tail group fragment; (D) 313, monoglyceride; (E) 369, cholesterol fragment; (F) 386, cholesterol molecular ion; (G) 551, diglyceride; (H) 706, DPPNME molecular ion; (I) 734, DPPC molecular ion. Note the differentiation of three membrane components via molecular ion detection (F, H, and I). 100-μm-wide fov; 1.6×10^{12} primary ions/cm^2.

Molecular differentiation of the three membrane components is achieved from the characteristic *m*/*z* peaks. The water clusters at high *m*/*z* are indicative of a hydrated sample thin enough not to experience significant charging due to ion beam analysis. The ability to detect these various headgroup, tail group, and molecular ion peaks illustrate that it is possible to distinguish a diverse group of phospholipids and steroids in situ with this technique.

Dynamical information related to interaction of phospholipid molecules during liposome collision or fusion events is acquired by the sample mixing protocol described above. Fast-freezing liposomes in the process of mixing provides an approach to determine phospholipids in different domains as well as the ability to capture dynamic events. By controlling mixing conditions, snapshot analyses of the molecular redistribution associated with fusion within liposomes are examined at various stages of interaction. The densities of liposome structures within the suspensions are intentionally kept low such that submonolayer samples are realized. Although submonolayer densities decrease the number of collisions that would induce fusion, these densities essentially eliminate superposition of structures between the two silicon layers. However, since TOF-SIMS is a surface-sensitive technique, this is only a concern for preparation-induced fusion artifacts and optical targeting.

Representative specific mass images for three different mixing outcomes (A−C, respectively) are shown in Figure 7. These represent, from left to right, C_3 hydrocarbons, phosphorylated headgroups, and cholesterol molecular ion, all overlaid on water. The phospholipid molecular ion mass is not as well represented across the image and is not shown. Several isolated and aggregated dipalmitoylphosphatidyldimethylethanolamine (DPPDME)/cholesterol liposomes that are in the same vicinity as a cluster of DPPC/cholesterol liposomes are shown in Figure 7A. The lower mass hydrocarbons are a good indicator of surface topography while the fragment ions of the phosphorylated headgroups indicate the chemical heterogeneity associated with spatially localized liposomes. The cholesterol molecular ion is clearly evident in each of the isolated liposomes.

Two liposomes in the process of fusion are shown in Figure 7B. The smaller liposome (~30-μm diameter on the left) is composed of DPPNME/cholesterol and the larger liposome (~60-μm diameter on the right) is composed of DPPC/cholesterol. The lower mass hydrocarbon intensity shows that the topography of the sample exhibits a contour that indicates the smaller liposome is recessed relative to the larger liposome. This arrangement is also apparent in the cholesterol signal. Reports from the 1970s have shown preferential distribution of cholesterol into phosphatidylcholine domains versus phosphatidylethanolamine domains,[46] and this effect might be evident here as well. Clearly, the image of the phosphorylated headgroup fragments depicts native phospholipid heterogeneity induced by two cell-size structures in the act of fusion. Interestingly, the image also shows a small but uniform mixing of both the DPPC and DPPNME into the other half of the fused liposomes, while the majority of each lipid remains in the original domain. The small amount of uniform mixing indicates nonrestricted diffusion of a small fraction of the phospholipids, whereas distinct domains of a much larger fraction of phospholipids remain apparently representing restricted diffusion. This observation is in accord with the early postulations from electron microscopy studies of discrete contact sites required for membrane fusion[47] versus random mixing. These contact sites have further been defined as an intermediate fusion structure in the membrane that is related to the hexagonal II phase.[48] Clearly, membrane domains are formed, at least transiently, during the fusion event. Furthermore, distribution and equilibration of the phospholipids throughout the structure occurs in more than one stage.

Molecular images representative of two liposomes that have completely fused into a single, homogeneous structure are shown in Figure 7C. The homogeneous redistribution of the molecular components completes the mixing sequence confirming that the chemical structure observed in Figure 7B is not an artifact of sample preparation such as phase segregation. Reproducibility of capturing dynamic membrane events depends not only on the occurrence of these discrete events but also on successful sample preparation techniques. For the chemical composition used for these studies, liposome compositions after longer mixing times (several minutes) are predominately evenly mixed. Conversely, liposome compositions observed in short mixing times are predominately not mixed, suggesting that sample preparation techniques are not inducing fusion in these submonolayer preparations. The images in Figure 7B are a representative case of the limited number ($n = 4$) of observed fusion events arrested during mixing. In summary, this suite of images shows that the phospholipid structure of liposomes during fusion proceeds through at least two stages. These stages include a discrete domain stage where diffusion into the other membrane structure appears limited through a contact point and eventually ends in a completely homogeneous fused liposome. During the initial fusion stage, a small fraction of the phos-

(46) Van Dijck, P. W. M.; De Kruijff, B.; Van Deenen, L. L. M.; De Gier, J.; Demel, R. A. *Biochim. Biophys. Acta* **1976**, *455*, 576−587.
(47) Hackenbrock, C. *Proc. Natl. Acad. Sci. U.S.A.* **1968**, *61*, 598−605.
(48) Van Venetie, R.; Verkleij, A. J. *Biochim. Biophys. Acta* **1981**, *645*, 262−269.

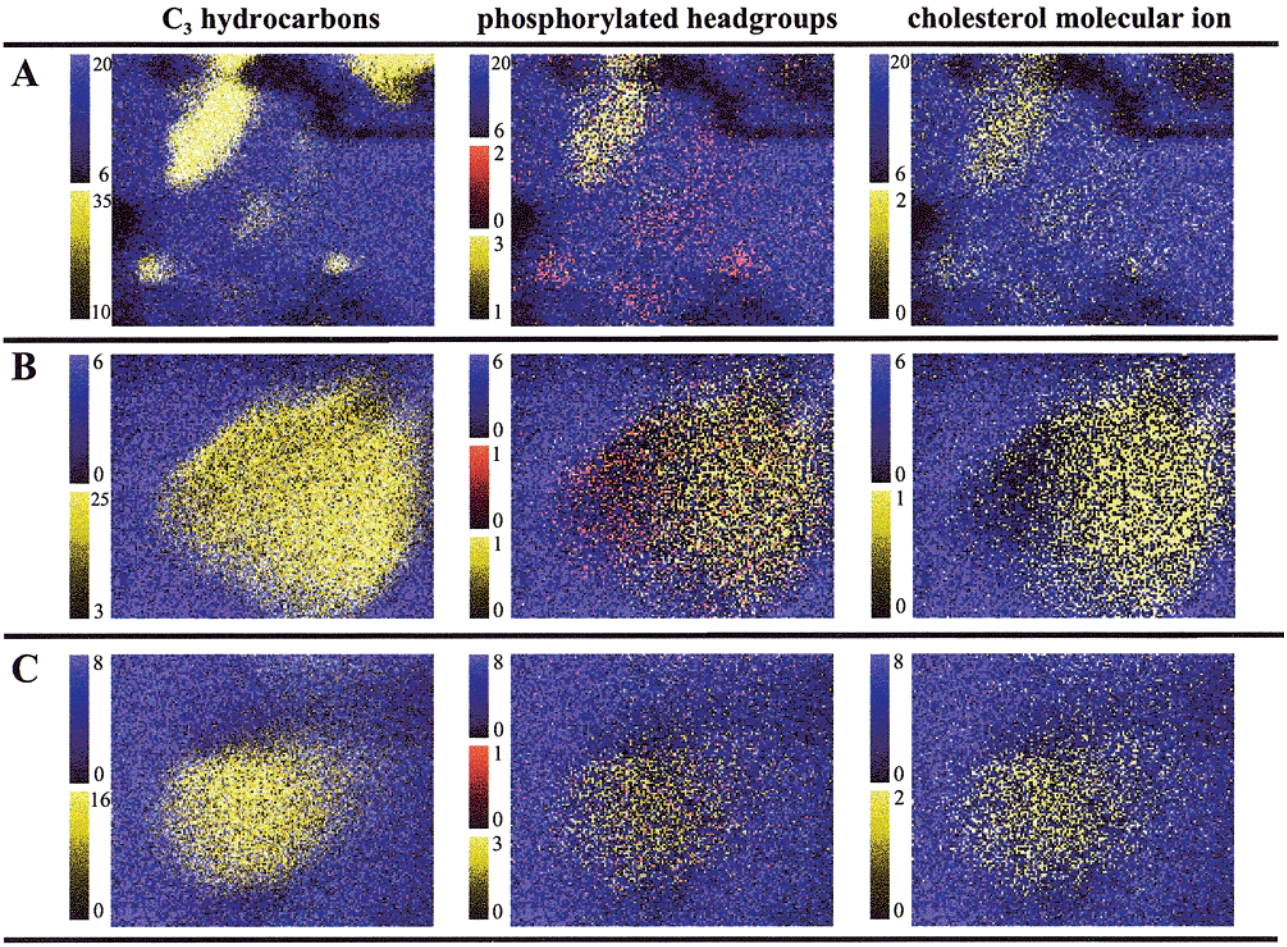

Figure 7. Positive ion TOF-SIMS images of freeze-fractured frozen-hydrated DPPC/cholesterol liposomes mixed with DPPDME/cholesterol or DPPNME/cholesterol liposomes. All images are overlaid with water (17.9−19.1 *m*/*z*; blue). Images, from left to right: C_3 hydrocarbons (40.9−43.3 *m*/*z*; yellow); phosphodimethylethanolamine headgroup (169.9−170.3 *m*/*z*; red) for (A) and phospho-*N*-monomethylethanolamine headgroup (155.9−156.3 *m*/*z*, red) for (B) and (C); phosphocholine headgroup (183.9−184.3 *m*/*z*, yellow); and cholesterol (384.1−387.2 *m*/*z*; yellow). All images are 152 × 148 pixels. Color equivalent intensity scales are left of the images with respective intensity ranges indicated. (A) DPPC/cholesterol liposomes mixed with DPPDME/cholesterol liposomes and frozen within 30 s of mixing. Significant mixing does not yet occurred. 200-μm-wide fov, 1.1×10^{12} primary ions/cm^2. (B) DPPC/cholesterol liposomes mixed with DPPNME/cholesterol liposomes and frozen within 60 s of mixing. Membrane fusion before major redistribution results in the heterogeneous distribution of membrane components; 100-μm-wide fov, 1.8×10^{13} primary ions/cm^2. (C) DPPC/cholesterol liposomes mixed with DPPNME/cholesterol liposomes and frozen within 120 s of mixing. Membrane fusion after major redistribution results in the homogeneous distribution of membrane components; 50-μm-wide fov, 6.5×10^{12} primary ions/cm^2.

pholipids mix between surfaces. Despite this, the majority of the lipids remain in separate sections of the membrane. These segregated domains appear to be similar to what is expected for membrane domains or "rafts" in cellular systems.

Conclusions

Development and optimization of freeze-fracture methodology specific to static TOF-SIMS molecular imaging of native chemical species of cellular membranes is reported. Freeze-fractured, frozen-hydrated model membranes demonstrate the special consideration of fracturing criteria that is required for molecule-specific TOF-SIMS imaging. A 15 °C temperature window is large enough to include fracturing extremes ranging from total water coverage to etching that disturbs the molecular spatial integrity measured by TOF-SIMS analysis. The fast-freezing times used in this study provide a relatively artifact free method of capturing membrane dynamics at discrete times during an event. It is apparent from the data shown that fusion of simple membranes involves formation of specific domains, initial distribution of a small portion of the phospholipids, and final redistribution and equilibration of the lipids to a homogeneous, fluid mosaic structure. The ability to image the heterogeneous molecular spatial distribution of membranes captured during dynamic events represents a unique approach in our development of membrane bioanalytical chemistry.

Acknowledgment. The authors acknowledge the National Institutes of Health, the National Science Foundation, and the Clare Boothe Luce Foundation for their funding. Thanks also goes to Rosemary Walsh, Angela Cannon, and Ed Basgall at the Pennsylvania State University for their help involving sample preparation.

JA992078P